The Plant Cell, Vol. 24: 2610–2623, June 2012, www.plantcell.org

Degradation of *Arabidopsis* CRY2 Is Regulated by SPA Proteins and Phytochrome A[W]

Guido Weidler,[a] Sven zur Oven-Krockhaus,[b] Michael Heunemann,[b] Christian Orth,[a] Frank Schleifenbaum,[b] Klaus Harter,[b] Ute Hoecker,[c] and Alfred Batschauer[a,1]

[a] Department of Plant Physiology, Faculty of Biology, Philipps-Universität, D-35032 Marburg, Germany
[b] Center of Plant Molecular Biology, Department of Plant Physiology, University of Tübingen, D-72076 Tuebingen, Germany
[c] Botanical Institute, University of Cologne, D-50674 Cologne, Germany

The UV-A/blue light photoreceptor crytochrome2 (cry2) plays a fundamental role in the transition from the vegetative to the reproductive phase in the facultative long-day plant *Arabidopsis thaliana*. The cry2 protein level strongly decreases when etiolated seedlings are exposed to blue light; cry2 is first phosphorylated, polyubiquitinated, and then degraded by the 26S proteasome. COP1 is involved in cry2 degradation, but several *cop1* mutants show only reduced but not abolished cry2 degradation. SUPPRESSOR OF *PHYA-105* (SPA) proteins are known to work in concert with COP1, and recently direct physical interaction between cry2 and SPA1 was demonstrated. Thus, we hypothesized that SPA proteins could also play a role in cry2 degradation. To this end, we analyzed cry2 protein levels in *spa* mutants. In all *spa* mutants analyzed, cry2 degradation under continuous blue light was alleviated in a fluence rate–dependent manner. Consistent with a role of SPA proteins in phytochrome A (phyA) signaling, a *phyA* mutant had enhanced cry2 levels, particularly under low fluence rate blue light. Fluorescence resonance energy transfer–fluorescence lifetime imaging microscopy studies showed a robust physical interaction of cry2 with SPA1 in nuclei of living cells. Our results suggest that cry2 stability is controlled by SPA and phyA, thus providing more information on the molecular mechanisms of interaction between cryptochrome and phytochrome photoreceptors.

INTRODUCTION

Cryptochromes constitute a family of UV-A/blue light photoreceptors that were first identified in plants (Ahmad and Cashmore, 1993; Batschauer, 1993) and subsequently found in animals, including humans, and in fungi and bacteria (Chaves et al., 2011). One peculiarity of cryptochromes is their high similarity in amino acid sequence and structure to DNA repair enzymes (DNA photolyases), which repair the two major UV-B lesions in DNA, the cyclobutane pyrimidine dimer, and the (6-4) pyrimidine-pyrimidone adduct (Sancar, 2003; Müller and Carell, 2009). Moreover, cryptochromes have the same essential flavin adenine dinucleotide (FAD) cofactor as DNA photolyase and most likely also the second antenna cofactor, methenyltetrahydrofolate (Malhotra et al., 1995; Hoang et al., 2008). Per definition, cryptochromes have no DNA repair activity, but several exceptions to this rule have been found, including the dual-function members of the cryptochrome/photolyase family from fungi (Bayram et al., 2008; Froehlich et al., 2010) and diatoms (Heijde et al., 2010).

The facultative long-day plant *Arabidopsis thaliana* encodes the cryptochromes cryptochrome1 (cry1), cry2, and cry3. cry1 plays an important role during deetiolation under white and blue light, and cry2 is involved in the transition to flowering under long-day conditions (Ahmad and Cashmore, 1993; Guo et al., 1998; El-Din El-Assal et al., 2001). cry3 is a DASH-type cryptochrome and is localized in organelles (Kleine et al., 2003). cry3, like other DASH-type cryptochromes, repairs cyclobutane pyrimidine dimers in single-stranded DNA (Selby and Sancar, 2006) and in loop structures of duplex DNA (Pokorny et al., 2008). A role of cry3 as a photoreceptor has not been demonstrated, although other members of the cry-DASH family very likely have photoreceptor function (Brudler et al., 2003; Brunelle et al., 2007; Froehlich et al., 2010).

cry1 and cry2 are involved in the differential expression of many genes (Ma et al., 2001; Folta et al., 2003; Ohgishi et al., 2004; Phee et al., 2007) and in the entrainment of the circadian clock (Somers et al., 1998). cry1 seems to shuttle between the nucleus and the cytosol (Cashmore et al., 1999; Yang et al., 2001; Wu and Spalding, 2007), whereas cry2 is constitutively localized in the nucleus (Guo et al., 1999; Kleiner et al., 1999).

cry2 regulates the induction of flowering under long-day conditions; it stabilizes the putative transcription factor CONSTANS (CO) (Yanovsky and Kay, 2002; Hayama and Coupland, 2004; Searle and Coupland, 2004; Valverde et al., 2004) and modulates the expression of another positively acting element of the photoperiodic pathway, *FLOWERING LOCUS T* (Liu et al., 2008). Also, cry1 has, in principle, the capacity to induce flowering since a gain-of-function mutation in *CRY1* was recently shown to strongly promote this process (Exner et al., 2010).

cry1 and cry2 are photoexcited by UV-A or blue light, which causes transition of the fully oxidized FAD in the ground state of the photoreceptor to the flavin neutral semiquinone in the lit state (Banerjee et al., 2007; Bouly et al., 2007). Upon

[1] Address correspondence to batschau@staff.uni-marburg.de.
The author responsible for distribution of materials integral to the findings presented in this article in accordance with the policy described in the Instructions for Authors (www.plantcell.org) is: Alfred Batschauer (batschau@staff.uni-marburg.de).
[W] Online version contains Web-only data.
www.plantcell.org/cgi/doi/10.1105/tpc.112.098210

photoexcitation, cry1 and cry2 become rapidly phosphorylated (Shalitin et al., 2002, 2003; Bouly et al., 2003), which is considered an important step in the signaling pathways of these photoreceptors (Shalitin et al., 2002; Liu et al., 2010). Phosphorylation of cry2 may also be the trigger for its rapid degradation, which occurs upon transition of etiolated seedlings to white or blue light but not to red light (Ahmad et al., 1998; Lin et al., 1998; Shalitin et al., 2002). However, under constant blue light, cry2 is present in seedlings and mature plants (Mockler et al., 2003), which indicates that cry2 is either not degraded completely or more cry2 is synthesized. Transcription of the *CRY2* gene, however, is not affected by blue light (Ahmad et al., 1998) but is under circadian control (Tóth et al., 2001). Upon irradiation of seedlings with blue light, cry2 also becomes polyubiquitinated, which is another signal for degradation by the proteasome, and results of cycloheximide and proteasome inhibitor studies clearly demonstrated that the decrease in the cry2 protein level is exclusively due to 26S proteasome–mediated degradation in the nucleus (Yu et al., 2007, 2009). Phytochromes seemed not to be involved in cry2 degradation (Yu et al., 2007), which suggests that photoexcitation of cry2 is required and sufficient for this process.

The protein CONSTITUTIVELY PHOTOMORPHOGENIC1 (COP1) interacts with cry1 and cry2 via their C-terminal extensions (CCT1 and CCT2, respectively) independent of light conditions (Wang et al., 2001; Yang et al., 2001). Moreover, overexpression of CCT1 or CCT2 causes a *cop1* phenotype (Yang et al., 2000). These results led to the conclusion that the photosensory N-terminal domain of cry1 and cry2 suppresses the respective CCT in the dark and in the activated state suppresses the E3 ubiquitin ligase activity of COP1 (Cashmore, 2003), thus preventing the degradation of activators of the light response by polyubiquitination, such as LONG HYPOCOTYL5 (HY5), LONG AFTER FR1, and LONG HYPOCOTYL IN FR1 (HFR1), which are subsequently degraded by the proteasome (Osterlund et al., 2000; Seo et al., 2003; Duek et al., 2004; Jang et al., 2005; Yang et al., 2005). The interaction of cry2 with COP1 is likewise important for the above-mentioned degradation of cry2, as demonstrated by higher cry2 levels in the *cop1* mutant under blue light compared with the wild type (Shalitin et al., 2002).

COP1 acts in visible light signaling in concert with related proteins of the SUPPRESSOR OF *PHYA-105* (SPA) protein family (Hoecker, 2005). The four members of the SPA protein family in *Arabidopsis* all have a common architecture, with a COP1-like WD repeat/β-propeller domain, a coiled-coil domain, and a kinase-like domain (Hoecker et al., 1999; Laubinger and Hoecker, 2003). All SPAs interact with each other and with COP1, likely forming a tetrameric complex via the respective coiled-coil domain (Hoecker and Quail, 2001; Saijo et al., 2003; Zhu et al., 2008). Single *spa* mutants essentially develop normally in the dark, whereas a *spa* quadruple mutant has a strong *cop* phenotype (Laubinger et al., 2004). Thus, SPAs function redundantly in suppressing photomorphogenesis in the dark. Single *spa* mutants, by contrast, show exaggerated light responses that are fully dependent on a functional phyA (Hoecker et al., 1998; Laubinger and Hoecker, 2003; Fittinghoff et al., 2006). Although this function of the various SPAs is redundant, they also have distinct roles during development. SPA1 and SPA2 have a major function during deetiolation, and SPA3 and SPA4 function is important in the adult stage (Laubinger et al., 2004; Fittinghoff et al., 2006).

Very recently it was shown by yeast two-hybrid and immunoprecipitation studies that cry2 and cry1 physically interact with SPA proteins. These interactions are specifically induced by blue light, showing preferential interaction of SPAs with the lit state of crys. Moreover, analysis of *spa*, *cry*, and *spa*/*cry* mutants showed that SPAs act downstream of cry in their respective signaling cascades to suppress COP1 activity and in consequence enhance levels of, for example, HY5 and CO. Despite these similarities in the role of SPAs in cry signaling, there are some striking differences between cry1 and cry2. cry2 interacts with its N-terminal photolyase-related domain with the N-terminal kinase-like domain of SPA1, but cry1 binds with its C-terminal domain (CCT1) to the WD repeat domain of SPA1. These different modes of interaction seem to have implications for how SPA1 affects the binding of COP1 to cry2 and cry1, as shown by yeast three-hybrid studies. Under blue light, SPA1 enhances binding of COP1 to cry2, whereas cry1 suppresses the COP1–SPA1 interaction (Lian et al., 2011; Liu et al., 2011; Zuo et al., 2011). This suggests that cry1 suppresses COP1 activity by attenuating its association with SPA1 possibly by competition for binding sites, whereas cry2 inhibits COP1 activity more directly by binding it stronger in the presence of SPA1 and forming a more stable SPA1-cry2-COP1 complex in blue light than in darkness.

The known role of COP1 in cry2 degradation, the coaction of SPAs with COP1, and the recently found direct interaction of cry2 with SPA1 (and less robust with SPA2-SPA4) led us to hypothesize that cry2 degradation might also be affected by SPAs. Here, we analyzed cry2 degradation in various *spa* mutants. cry2 degradation in *spa* mutants was much lower than in the wild type, particularly under very low and low blue light fluence rates. Consistent with a role of SPAs in phyA signaling, the fluence rate–dependent cry2 degradation decreased in a *phyA* mutant. Moreover, using fluorescence resonance energy transfer–fluorescence lifetime imaging microscopy (FRET-FLIM), we demonstrate a direct physical interaction of cry2 with SPA1 in the nucleus of living cells. Thus, degradation of cry2 is mediated by COP1 in concert with SPAs similarly if not identically as seen with the transcription factors HY5 and HFR1.

RESULTS

Degradation of CRY2 Is Diminished in *spa* Mutants

cry2 is rapidly degraded in etiolated *Arabidopsis* seedlings when exposed to continuous blue light (Ahmad et al., 1998; Lin et al., 1998; Shalitin et al., 2002). Since COP1 plays a role in cry2 degradation (Shalitin et al., 2002), SPA proteins work in concert with COP1 (Hoecker, 2005), and both COP1 and SPAs physically interact with cry2 (Wang et al., 2001; Zuo et al., 2011), we questioned whether SPA proteins have a function in cry2 degradation. To this end, we studied the kinetics of cry2 degradation in etiolated Columbia wild-type and *spa1/2/4* triple mutant seedlings exposed to continuous blue light. cry2 protein levels

were quantified using a Li-Cor Odyssey infrared imaging system, which allowed reliable detection of an infrared fluorophore-labeled secondary antibody that recognizes the cry2-specific antibody. cry2 protein levels were normalized here and in subsequent experiments to the α-tubulin signal obtained from the same immunoblot (Figure 1B); the cry2 protein levels were in the linear range for both the cry2 and the α-tubulin signals (see Supplemental Figure 1 online). The specificity of the anti-cry2 antibody was again confirmed with extracts obtained from *cry2* mutant plants that showed no cry2 signal on immunoblots (Figure 1C). A very rapid and strong blue light–induced decrease in cry2 protein levels was observed in the wild type, with essentially no detectable protein remaining after 180 min of irradiation, even though the applied fluence rate of blue light (λ_{max} 471 nm; 15 μmol m^{-2} s^{-1}) was only moderate (Figure 1A). Likewise, cry2 rapidly degraded in the *spa1/2/4* mutant seedlings kept under the same light conditions (Figure 1A), but the extent of cry2 degradation in the *spa1/2/4* mutant was lower than in the wild type. This resulted in significantly higher cry2 protein levels in the *spa1/2/4* mutant than in the wild type at 15, 90, and 120 min after the onset of irradiation. Albeit significant, the differences in cry2 protein levels between the wild type and the *spa1/2/4* mutant were not very great under the fluence rate of blue light used in this experiment.

Since cry2 degradation is fluence rate dependent (Ahmad et al., 1998; Lin et al., 1998; Yu et al., 2007), we analyzed the dose response of cry2 degradation in the wild type and *spa* mutants (all in a Columbia background). In these studies, we included the *spa1* single mutant, all combinations of *spa* triple mutants, and the *spa1/2/3/4* quadruple mutant that lacks all SPA proteins. Particularly under low fluence rates of blue light (0.01 to 1 μmol m^{-2} s^{-1}), the degradation of cry2 was strongly reduced in all *spa* mutants tested (Figure 2; for original data, see Supplemental Figure 2 online). However, under low fluence rates, the reduction in cry2 degradation in the *spa1/2/3* triple was less pronounced than in the other mutants, and under higher fluence rates, the cry2 level was higher in the *spa1/2/3* triple than in the wild type and the other *spa* mutants. Since the cry2 levels in darkness, when normalized to the α-tubulin signal as a loading control, were essentially the same in the wild type and the *spa* mutants (see Supplemental Figure 2 online), the higher level of cry2 in the *spa* mutants is due to reduced degradation during irradiation and not to increased synthesis.

The decrease in cry2 protein levels of blue light–irradiated seedlings was previously shown to be caused by enhanced protein degradation and not by a decrease in *CRY2* transcript levels (Ahmad et al., 1998). To confirm that the same holds true under our experimental conditions, we analyzed *CRY2* transcript levels by quantitative RT-PCR. There was no significant difference in *CRY2* transcript levels comparing dark-grown and low fluence rate blue light–treated wild type, *spa1/2/4*, and *phyA* mutant seedlings (see Supplemental Figure 3 online). Compared with dark-grown seedlings, when seedlings were treated for 2 h with a higher fluence rate of blue light (30 μmol m^{-2} s^{-1}), we observed some decrease in *CRY2* transcripts. However, this decrease was again the same for all genotypes. We conclude from this result that neither SPAs nor phyA has an effect on the level of *CRY2* transcripts.

In line with the conclusion that the amount of cry2 protein is mainly regulated at the protein level, Yu et al. (2007) found that cry2 degradation in the Columbia-0 (Col-0) ecotype is inhibited by the proteasome inhibitor MG132. Using even higher doses of blue light and a combination of different proteasome inhibitors, we found a similar reduction in cry2 degradation by the proteasome inhibitors for all ecotypes applied in our study (see Supplemental Figure 4 online). This confirms again that the decrease in cry2 protein levels seen under blue light irradiation is the result of a proteolytic degradation occurring in all *Arabidopsis* accessions tested here.

CRY2 Degradation Is Controlled by phyA

In contrast with the effect of blue light, irradiation of seedlings with red light has essentially no effect on cry2 levels; therefore, it was concluded that cry2 degradation depends exclusively on blue light (Ahmad et al., 1998; Lin et al., 1998; Yu et al., 2007). We found the same lack of effect of red light on cry2 levels in an experiment using the same fluence rates of red light that we used for the blue light experiments (0.01 to 30 μmol m^{-2} s^{-1}; see Supplemental Figure 5 online). Similarly, far-red light at high fluence rates (15 and 30 μmol m^{-2} s^{-1}) did not result in any degradation of cry2 (see Supplemental Figure 5 online). These results are also in line with previous data (Yu et al., 2007) showing that activation of phytochromes alone has no effect on cry2 levels, independent of the phytochrome response modes analyzed (very low fluence response, low fluence response, far-red high irradiance response). Moreover, our data are consistent with the point of view that photoactivation of cry2, which occurs only with wavelengths below 500 nm (Banerjee et al., 2007), is required and sufficient for cry2 degradation.

SPA proteins are involved in the signaling cascade of phyA during the deetiolation process (Laubinger et al., 2004; Fittinghoff et al., 2006). Considering the above shown role of SPAs in cry2 degradation, we investigated whether phyA has a role in cry2 degradation. Surprisingly, much less cry2 was degraded in the *phyA* mutant under very low and low fluence rates of blue light (0.01 to 1 μmol m^{-2} s^{-1}). This effect was nearly as pronounced as that observed in the *cop1* mutant (Figure 3). At higher fluence rates, the difference between the wild type and the *phyA* mutant was not significant; the *cop1* mutant had higher but not significantly different cry2 levels than the wild type under high fluence rates of blue light (Figure 3). Our data show that there is a very low fluence response of phyA, resulting in enhanced cry2 degradation, which occurs only when cry2 itself is photoactivated by blue light. This finding provoked us to analyze whether phyB also promotes cry2 degradation. However, the observed cry2 levels in the *phyB* mutant were not statistically different from those of the wild type (Figure 4).

Surprisingly, the extent of cry2 degradation under blue light fluence rates of up to 1 μmol m^{-2} s^{-1} was much lower in the Landsberg *erecta* (L*er*) wild type (Figure 4) than in the Col-0 wild type (Figure 3). For example, irradiation of the Col-0 wild type with blue light for 2 h at 0.01 μmol m^{-2} s^{-1} resulted in about a 60% lower amount of cry2 protein compared with the dark level, whereas the same irradiation of L*er* wild type caused only a 25% lower amount. This generally weaker decrease in cry2

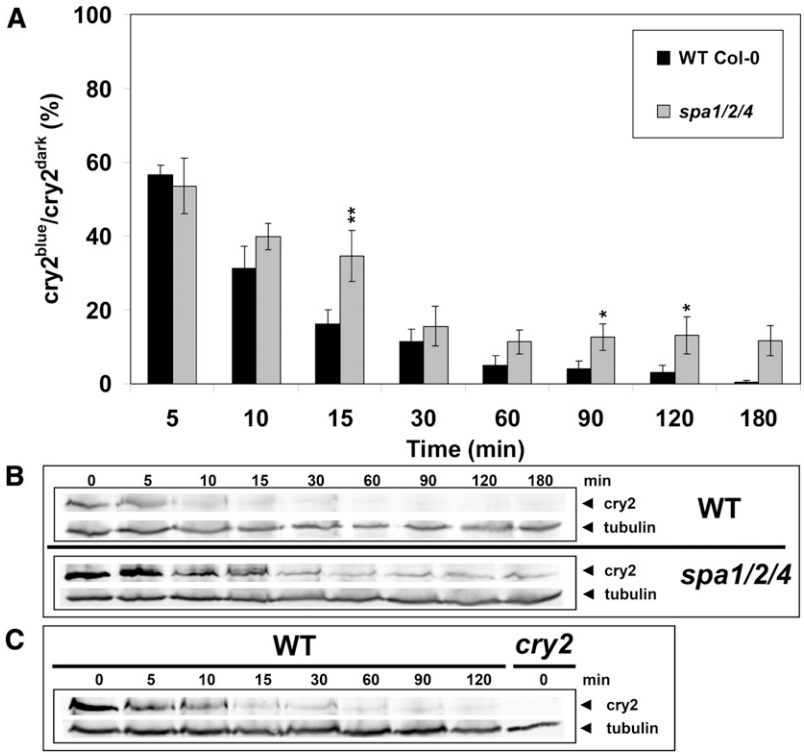

Figure 1. Time Course of CRY2 Degradation in Dark-to-Blue Light Transition in Wild-Type and *spa1/2/4* Mutant Seedlings.

(A) Time course of cry2 degradation under constant blue light (λ_{max} = 471 nm, 15 μmol m^{-2} s^{-1}). The cry2 levels were normalized to the α-tubulin signal and to the cry2 signal of 96-h-old dark-grown seedlings of the same genotype. The wild type (WT) and the *spa1/2/4* mutant were in the Col-0 background. Given are mean values of three independent experiments and SE. Asterisks indicate *t* test analysis for statistically significant differences between the wild type and the *spa1/2/4* mutant under the same light conditions, with P values ≤ 0.05 (*) or ≤ 0.01 (**).

(B) Representative immunoblot of the kinetics shown in **(A)**. The blot was probed with anti-cry2 and antitubulin antibodies in parallel.

(C) Representative immunoblot showing the degradation of cry2 in etiolated wild-type seedlings upon exposure to blue light (same wavebands and fluence rate as in **[A]** and **[B]**). The blot was probed as in **(B)**. Included was a protein sample from dark-grown 4-d-old *cry2* mutant seedlings to confirm the specificity of the anti-cry2 antibody.

levels in the L*er* ecotype under low fluence rates of blue light might explain the similarly less pronounced effect of the *phyA* mutation in the L*er* background (Figure 4) compared with the Col-0 background (Figure 3). cry2 degradation under low fluence rates of blue light is even less pronounced in the Rschew (RLD) accession compared with Col-0 and L*er* accessions (see Supplemental Figure 6 online). Likewise, *spa1*, *phyA*, and *spa1/phyA* mutants in the RLD background behaved like the wild type in the dose-dependent degradation of cry2 (see Supplemental Figure 7 online). The reason for this discrepancy between different accessions is not clear yet. However, the lower sensitivity of L*er* and RLD accessions compared with Col-0 is not the result of different mechanisms of downregulation of cry2 protein levels since plants of all accessions showed a qualitatively similar response to the proteasome inhibitors (see Supplemental Figure 4 online). Moreover, no significant difference was seen between Col-0, L*er*, and RLD accessions in their dose–response curves of hypocotyl growth inhibition under blue light (see Supplemental Figure 8 online). Thus, the different sensitivities of these three *Arabidopsis* accessions against blue light are not a general feature but could be specific for the degradation of cry2.

CRY2 Directly Interacts With SPA1 in Nuclei of Living Cells

Recently, it has been shown that cry2 colocalizes with SPA1 in nuclei of fixed *Arabidopsis* cells (Zuo et al., 2011) and in nuclei of onion (*Allium cepa*) epidermal cells (Lian et al., 2011). Also, these authors used coimmunoprecipitation (Co-IP) and yeast two-hybrid interaction techniques to show that cry2 interacts with SPA1. Moreover, it was demonstrated by yeast two-hybrid studies that SPA2-SPA4 also interact with cry2; however, SPA1 showed the most robust interaction among all four SPA proteins (Zuo et al., 2011). Although these data clearly show that cry2 interacts with all four SPAs, it cannot be excluded that in nuclei of living plant cells some of these interactions are mediated by adaptor proteins such as COP1. We therefore applied FRET-FLIM to analyze more rigorously direct interactions between cry2 and all members of the SPA quartet. As a positive control, we used CRYPTOCHROME-INTERACTING BASIC-HELIX-LOOP-HELIX PROTEIN1 (CIB1), which has been shown to bind to photoactivated cry2 in living plant, yeast, and mammalian cells (Liu et al., 2008; Kennedy et al., 2010). To this end, full-length cry2 and CIB1 were fused to green fluorescent protein

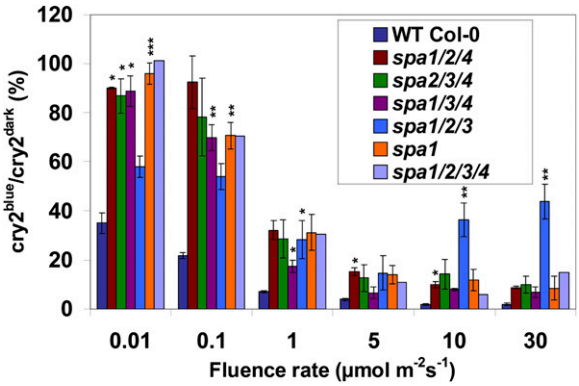

Figure 2. Fluence Rate–Dependent Degradation of CRY2 in Wild-Type and *spa* Mutant Seedlings.

Etiolated seedlings (96-h-old, all in Col-0 background) were exposed to blue light (λ_{max} = 471 nm) for 120 min at the indicated fluence rates. Given are mean values and SE of relative cry2 levels of seedlings exposed to blue light ($cry2^{blue}$) compared with the cry2 level of seedlings of the same genotype kept in the dark ($cry2^{dark}$ = 100%) and normalized to the α-tubulin signals of each probe. Data are from three biological replicates, except for the *spa1/2/3/4* mutant, which was measured only once. Asterisks indicate *t* test analysis for statistically significant differences between the wild type and the respective mutant under the same conditions, with P values ≤ 0.05 (*), ≤ 0.01 (**), or ≤ 0.001 (***). WT, the wild type.

(GFP) or red fluorescent protein (RFP) either at the N or C terminus, respectively. In the case of SPA1-SPA4, full-length proteins were fused to the fluorescent proteins only at their N terminus since C-terminal fusions are not tolerated by these proteins. Genes encoding these fusions were introduced into light-grown *Nicotiana benthamiana* leaves by *Agrobacterium tumefaciens* infiltration. Expression of full-length fusion proteins was verified by immunoblot analysis (see Supplemental Figure 9 online). As shown in Figure 5, cry2, CIB1, and all four SPAs localized to nuclei as additionally verified using the mCherry-NLS reporter (Wanke et al., 2011). Moreover, the pictures from the merged GFP and RFP channels showed that cry2 colocalizes with CIB1 and all four SPAs. This supports previous findings for the colocalization of cry2 with CIB1 (Kennedy et al., 2010) and with SPA1 (Lian et al., 2011; Zuo et al., 2011) but does not prove unambiguously a direct interaction of cry2 with all SPAs. To test this in greater detail, we applied FRET-FLIM. This technique allows the detection of direct protein–protein interactions of fluorophore-labeled partners in living cells, which results in shorter fluorescence lifetimes of the donor fluorophore depending on the rate of energy transfer to the acceptor fluorophore (Harter et al., 2012). The results of these measurements are shown in Figure 6. As negative controls (no energy transfer), we used the fluorescence lifetimes of the GFP-SPA1 single transformant and the GFP-SPA1/mCherry-NLS double transformant, which were in the same range of 2.30 nano seconds (ns). The positive controls (GFP-CIB1/RFP-CRY2 and GFP-CIB1/CRY2-RFP) showed significantly shorter lifetimes compared with the negative controls between 1.90 and 2.04 ns. This result clearly confirms a direct physical interaction between cry2 and CIB1 in the nuclei of living plant cells. All three combinations tested for the cry2-SPA1 interaction (GFP-SPA1/RFP-CRY2, GFP-SPA1/CRY2-RFP, and RFP-SPA1/CRY2-GFP) showed, in comparison to the negative controls, significantly reduced fluorescence lifetimes in the range between 1.90 and 2.00 ns. Thus, the rate of energy transfer in the cry2-SPA1 combination is nearly the same as in the cry2-CIB1 interaction. Thus, cry2 interacts directly with SPA1 in the nucleus.

Since the interaction of cry2 with all members of the SPA quartet was demonstrated by yeast two-hybrid interaction studies (Zuo et al., 2011), we were interested in applying FRET-FLIM to test whether these interactions also occur in nuclei of living plant cells. Since in the FRET-FLIM assay there was robust interaction of cry2 with SPA1 detectable independent from which fluorescent protein (GFP or RFP) was fused to cry2 and whether this fusion was made at its N- or C terminus, we tested only the GFP-SPA2-4/RFP-cry2 combinations. None of these combinations led to significantly shorter fluorescence lifetimes compared with the negative controls (Figure 6), although all fusion proteins were expressed to similar levels (Figure 5; see Supplemental Figure 9 online). Thus, these studies provided no proof for a direct interaction of cry2 with SPA2-4 in living plant cells. To verify these data, we conducted in vitro pull-down experiments using in vitro–transcribed and translated SPA1-4 proteins and recombinant, affinity-purified cry2 expressed in insect cells. The expression of cry2 in insect cells allows the production of photoactive photoreceptor (Banerjee et al., 2007). The cry2 sample used in our studies had a correctly bound FAD cofactor and showed a normal photocycle (see Supplemental Figure 10A online). As a negative control in our pull-down experiments, we used recombinant and functional *Escherichia coli* DNA photolyase (see Supplemental Figure 10A and Supplemental References 1 online) as a bait because cry2 and photolyase are structurally highly similar flavoproteins, but with

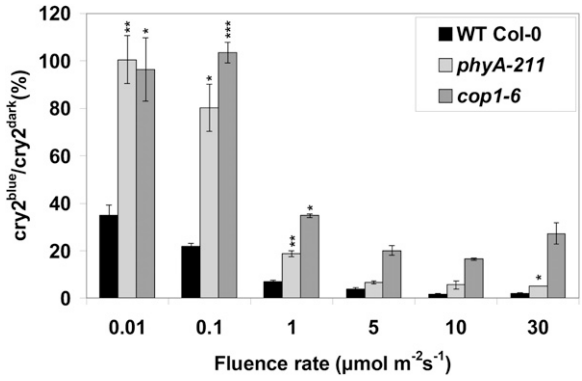

Figure 3. Fluence Rate–Dependent Degradation of CRY2 in Wild-Type, *phyA-211*, and *cop1-6* Mutant Seedlings.

Etiolated seedlings (96-h-old, all in the Col-0 background) were exposed to blue light (λ_{max} = 471 nm) for 120 min at the indicated fluence rates. Data were acquired from the immunoblots and normalized as described in Figure 2. Given are mean values and SE of three independent experiments; asterisks indicate *t* test analysis for statistically significant differences, with P values ≤ 0.05 (*), ≤ 0.01 (**), or ≤ 0.01 (***). WT, the wild type.

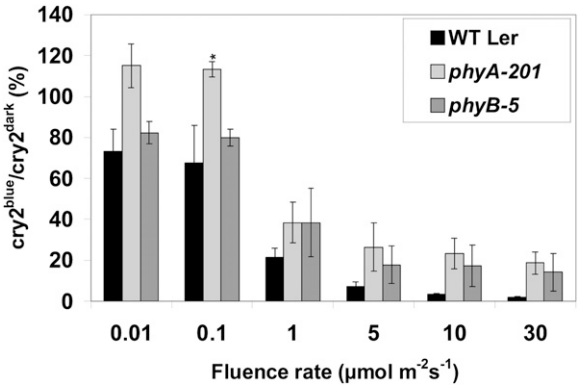

Figure 4. Fluence Rate–Dependent Degradation of CRY2 in Wild-Type, *phyA-201*, and *phyB-5* Mutant Seedlings.

Etiolated seedlings (96-h-old; all in the L*er* background) were exposed to blue light (λ_{max} = 471 nm) for 120 min at the indicated fluence rates. Data were acquired from the immunoblots and normalized as described in Figure 2. Given are mean values and SE of three independent experiments; asterisks indicate *t* test analysis for statistically significant differences, with P values ≤ 0.05 (*). WT, the wild type.

completely different biological functions. The recombinant cry2 and *E. coli* DNA photolyase baits carried a 6×His-tag, which allowed both proteins to be specifically and quantitatively immunoprecipitated with the same anti-His-tag antibody (see Supplemental Figures 10B and 10C online). The bait and prey proteins and all following steps were incubated either under white light or under safe red light to test whether the interaction is light dependent. For SPA2 and SPA3, nearly identical signals were obtained in the white and red light assays independent of the presence of cry2 (Figures 7A and 7B). We interpret these signals obtained in the absence of cry2 as unspecific binding of SPA2 and SPA3 to the His-tag antibody and/or the protein G magnetic beads. In contrast with SPA2 and SPA3, no unspecific signals were obtained for SPA1 and SPA4. The addition of cry2 to the assays kept in white light resulted in clear signals, which indicated that these two SPA proteins bind to cry2 (Figure 7A). When the same assays were performed under red light, the results were very similar (Figure 7B). Thus, SPA1 and SPA4 seemed to interact with cry2 in a light-independent fashion.

To confirm the significance of these results, we performed control experiments with proteins already known to interact directly with cry2. As mentioned above, COP1 interacts with cry2 independent of light (Wang et al., 2001). The results of our Co-IP experiments with recombinant cry2 and in vitro–transcribed and translated COP1 are in agreement with this finding (Figure 7C). Another protein that interacts with cry2 is CIB1, a basic helix-loop-helix protein (Liu et al., 2008). Indeed, we detected CIB1 binding to cry2 under white light, but also under red light, which suggested a light-independent interaction (Figure 7D). This result was unexpected since CIB1 was reported not to interact with cry2 under red light (Liu et al., 2008). However, closer analysis of our results indicated that the coprecipitated fraction of CIB1 was higher under white light than under red light, which is indicative of a higher affinity of CIB1 to the lit state of cry2 than to its dark state. The reliability of our Co-IP experiments was further confirmed in negative controls using *E. coli* DNA photolyase as the bait protein, which did not bind CIB1 or SPA1 (Figure 7E).

DISCUSSION

In *Arabidopsis*, the photoreceptors phyA and cry2 are rapidly degraded under red and blue light, respectively (Clough and Viestra, 1997; Ahmad et al., 1998; Lin et al., 1998; Clough et al., 1999; Sharrock and Clack, 2002; Yu et al., 2007). More recent data have shown that other photoreceptors that were considered to be light stable, such as phyB, are also considerably degraded in the light (Leivar et al., 2008; Jang et al., 2010).

The light-labile photoreceptors phyA and cry2 play the most important roles in photoperiodic flowering (Guo et al., 1998; Mockler et al., 2003; Hayama and Coupland, 2004; Searle and Coupland, 2004), which suggests that the coupling of activation and degradation (desensitization) by phosphorylation of these receptors is important for their role as daylength sensors (Mockler et al., 2003). However, such a conclusion requires further studies since, for example, a gain-of-function mutant of *cry1* (*cry1*-L407F), which does not affect cry1 protein levels, strongly promotes flowering (Exner et al., 2010), although the exact mechanism how cry1 could induce flowering is currently unknown. Thus, cry1 also can principally function as an activator of the floral transition even though its protein abundance essentially does not fluctuate (Mockler et al., 2003). Likewise, oscillation of the cry2 protein level is particularly pronounced under short-day conditions, while barely detectable under long-day conditions, which promote flowering (Mockler et al., 2003).

The cry2 degradation mechanism has been studied in detail. The decrease in cry2 protein level observed in etiolated seedlings exposed to light is mainly, if not exclusively, caused by degradation of the protein. This was shown by measurements of *CRY2* transcript levels, which remained the same under dark and light conditions, as well as by inhibition of protein de novo synthesis using cycloheximide, which had no effect on the decrease of cry2 protein upon blue light exposure of the seedlings (Ahmad et al., 1998). We confirmed these results by showing that the *CRY2* transcript levels remained essentially constant under low fluence rate blue light and had only a 40 to 50% reduction under the high light. Most importantly, the *spa* and *phyA* mutants had the same *CRY2* transcript levels as the wild type (see Supplemental Figure 3 online). cry2 is degraded only under blue light in a fluence rate–dependent fashion (Ahmad et al., 1998; Lin et al., 1998); other light qualities are ineffective. Our data support these results (see Supplemental Figure 5 online). However, in contrast with the study of Yu et al. (2007), we observed a clear effect of phyA on cry2 degradation under blue light: The *phyA* mutant, particularly in the Col-0 background, had significantly higher cry2 levels than the wild type under very low and low fluence rates of blue light (Figure 3). The apparent inconsistency between our data and those previously reported can be explained by the blue light fluence rate (15 μmol m^{-2} s^{-1}) used to study the effect of phyA and other phytochromes on cry2 protein levels. The fluence rate used in the study of Yu et al.

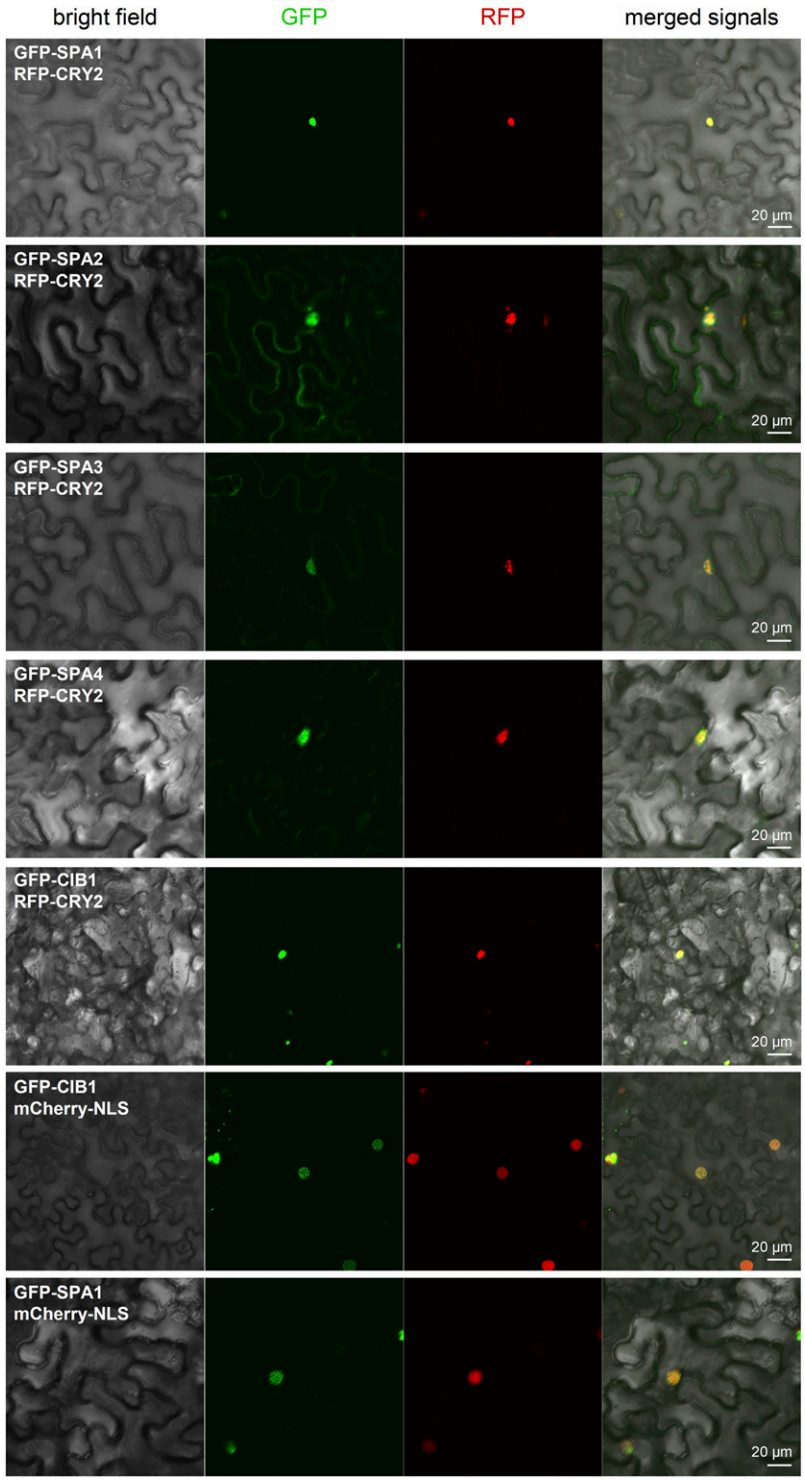

Figure 5. Nuclear Colocalization of CRY2 with SPAs and CIB1.

Confocal laser scanning microscopy of GFP/RFP fusion proteins coexpressed in tobacco leaves. Nuclear colocalization of cry2 with CIB1 as well as with all members of the SPA quartet is shown. Bars = 20 μm.

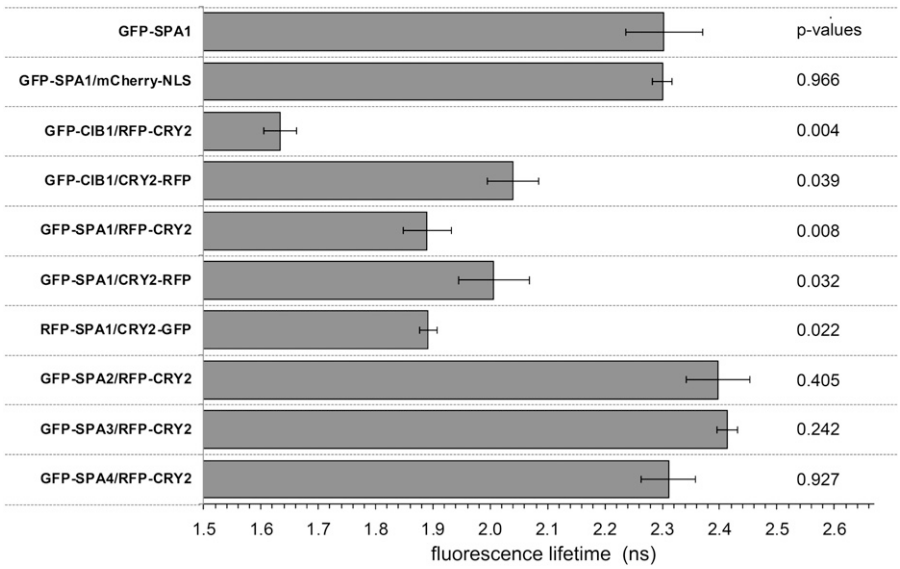

Figure 6. Fluorescence Lifetime Measurements Show Interaction of CRY2 with SPA1 and CIB1 in Nuclei of Living Plant Cells.

In vivo GFP fluorescence lifetime measurements of different GFP/RFP fusion protein combinations. N-terminal or C-terminal tagged cry2 fusion proteins were coexpressed with N-terminal GFP/RFP fusion proteins of CIB1 or SPA1-SPA4. Fluorescence lifetime measurements of GFP-SPA1 and GFP-SPA1/mCherry-NLS served as negative controls. The combination of GFP-CIB1 with either RFP-CRY2 or CRY2-RFP served as positive controls. Given are mean values and SE of three independent measurements; P values indicate *t* test analysis for statistical significant differences.

(2007) was in a range where we also could not observe any significant difference between the *phyA* mutant and the wild type. Thus, the effect of phyA on blue light–induced cry2 degradation is only evident under low blue light fluence rates. Several other blue light responses mediated by phyA have been reported (Shinomura et al., 1996; Mockler et al., 2003; Lariguet and Fankhauser, 2004). We also observed a strong effect of phyA on hypocotyl growth inhibition under blue light when we compared the *cry1 cry2* mutant with the *phyA cry1 cry2* mutant (see Supplemental Figure 11 online). Thus, blue light signaling by phyA induces a number of blue light responses, which include deetiolation as well as cry2 degradation. Taken together, our data emphasize that crosstalk between phytochrome and cryptochrome results in a direct regulation of cry2 degradation by phyA.

cry2 is phosphorylated and ubiquitinated before degradation in the nucleus in the 26S proteasome (Yu et al., 2007, 2009). Since the level of cry2 remaining, for example, after 2 h irradiation with 35 μmol m^{-2} s^{-1} of blue light, is much higher in *cop1-4* and *cop1-6* mutants than in wild-type seedlings but still significantly lower than in the dark controls (Shalitin et al., 2002), COP1 is clearly involved in cry2 degradation. cry2 degradation is only hampered but not completely abolished in *cop1-4* and *cop1-6*, which could be explained by these alleles not being null (i.e., that some residual COP1 activity remains in these mutants). However, the same authors stated that even in the *cop1-5* null mutant, some cry2 was degraded. Thus, COP1 function could be redundant with other E3 ubiquitin ligase components. Indeed, mutants defective in several SPAs, in particular the *spa* quadruple mutant, had a moderate to severe *cop* phenotype. We therefore investigated whether cry2 degradation is affected in *spa* mutants. Under high fluence rates of blue light, we observed essentially no difference between wild-type and *spa* mutant seedlings. By contrast, we observed significantly higher cry2 levels in the *spa* mutants than in the wild type under very low and low fluence rates of blue light (Figure 2). This shows unequivocally that SPA proteins are involved in cry2 degradation and moreover suggests that COP1 acts in concert with SPA proteins in cry2 degradation. It is tempting to speculate that the residual cry2 degradation observed in the *cop1-5* and *spa*-quadruple mutants may be due to the respective other component in the COP1/SPA complex operating in these mutants. To test this possibility, a *cop1-5 spa* quadruple mutant needs to be examined. Alternatively, an additional ubiquitin ligase might operate in blue light–induced cry2 degradation. A further explanation for the increased cry2 protein levels in *spa* mutants under low fluence rates of blue light could be the result of a downregulation of COP1 when SPA proteins are lacking. However, just the opposite was observed, namely, increased COP1 levels compared with the wild type in particular for *spa1/2*, *spa1/2/3*, *spa1/2/4*, and *spa2/3/4* (Zhu et al., 2008). Thus, SPAs do not have an accessory function for COP1 but seem to be essential components for the effective degradation of cry2 under low fluence rate blue light.

Since even the *spa1* single mutant had reduced cry2 degradation to the same extent as the triple and the quadruple mutants, SPA1 could have a dominant role in this process. However, the *spa2/3/4* mutant, which has SPA1, is likewise affected in cry2 degradation. Therefore, deletion of one SPA can be compensated for at least in part by others, and there is no strict requirement for SPA1 for cry2 degradation under high fluence rates of blue light, since even the *spa* quadruple mutant

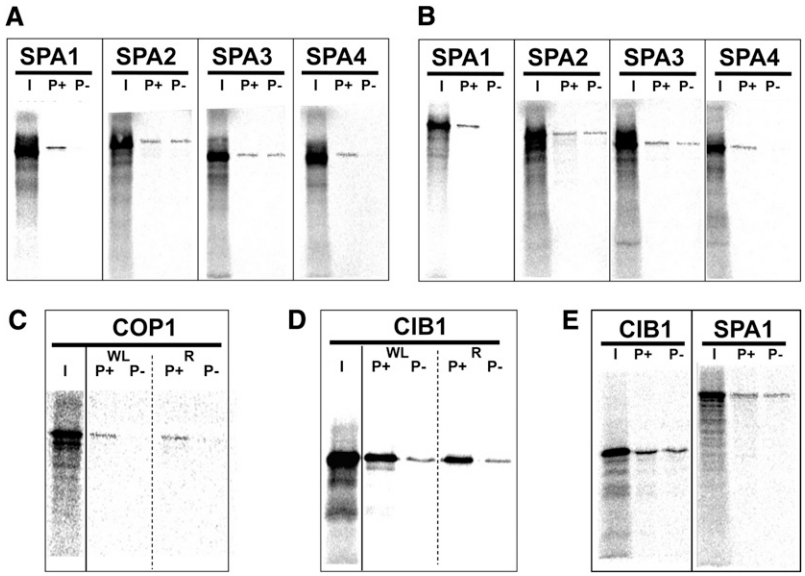

Figure 7. Co-IP of Recombinant His-Tagged CRY2 with Various Radiolabeled Prey Proteins.

(A) and **(B)** Co-IP assays with cry2 and in vitro–transcribed and translated [^{35}S]Met-labeled SPA proteins. The assays were kept continuously under white light **(A)** to keep cry2 active or under red light **(B)** to avoid cry2 activation. I, 2 μL aliquot of the respective TnT reaction; P+, pellet fraction from assay where cry2 was included; P-, pellet fraction from assay without cry2.

(C) and **(D)** Co-IP assays of cry2 with COP1 **(C)** and CIB1 **(D)**. Assays were performed as in **(A)** and **(B)**. R, assays were kept under continuous red light; WL, assays were kept under continuous white light.

(E) Instead of cry2 as the bait protein, *E. coli* photolyase was used in a Co-IP assay with CIB1 and SPA1 as prey proteins. Assays were performed under continuous white light. None of the prey proteins CIB1 and SPA1 that physically interacted with cry2 specifically bound to *E. coli* photolyase.

has under these conditions essentially the same cry2 level as the wild type. Somewhat surprising is the behavior of the *spa1/2/3* mutant since it has, compared with the other *spa* mutants, lower cry2 levels under low light conditions but higher levels under high light conditions (Figure 2). This result suggests that SPA proteins affect each other's activity in a complex manner that itself is fluence rate dependent. Despite their redundant roles, the SPAs also have specific functions. SPA1 and SPA2 are the prominent players in the suppression of photomorphogenesis in the dark, and SPA3 and SPA4 dominate in light-grown seedlings and plants (Laubinger et al., 2004; Fittinghoff et al., 2006). Considering that the blue light–induced degradation of cry2 is part of the deetiolation process, one could expect that cry2 degradation is preliminarily influenced by SPA1 and SPA2. The strong effect seen in the *spa1* single mutant indeed suggests that SPA1 has a prominent role in cry2 degradation. However, SPA1 alone is unable to mediate efficient cry2 degradation since the *spa2/3/4* mutant is likewise hampered in this process. The same holds true for SPA2 as seen with the *spa1/3/4* mutant, which also has reduced cry2 degradation under low blue light fluence rates (Figure 2). Likewise, neither SPA3 (*spa1/2/4* mutant) nor SPA4 (*spa1/2/3* mutant) alone is completely sufficient to mediate the degradation of cry2, although the reduced response seen for the *spa1/2/3* mutant under low fluence rates of blue light indicates some important role of SPA4 in this process. In summary, our results show functional redundancy among all SPA proteins in cry2 degradation. As deduced by elimination from the results of experiments with the triple mutants and the *spa1* single mutant, it seems likely that SPA1 and SPA4 play the most important role in cry2 degradation.

So far, SPA proteins have been considered to operate in concert with COP1 by direct interaction with COP1 (Hoecker and Quail, 2001; Saijo et al., 2003; Laubinger et al., 2004). As a result of this interaction, the activity of COP1 as an E3 ubiquitin ligase may be enhanced (Seo et al., 2003), although the opposite effect has been observed when full-length SPA1 and other E1 and E2 enzymes have been used (Saijo et al., 2003). Considering the similar domain structure of COP1 and SPA proteins and the direct interaction of COP1 with cry2 (Wang et al., 2001), a direct interaction of cry2 also with SPAs is not unlikely. Indeed, three recent publications demonstrated a direct physical interaction of cry2 and cry1 preferentially with SPA1 (and less robust with SPA2-SPA4) by yeast two-hybrid interaction studies (Lian et al., 2011; Liu et al., 2011; Zuo et al., 2011). Colocalization of cry2 and cry1 with all members of the SPA quartet in nuclei of plant cells as well as Co-IPs from plant extracts strongly suggested that direct interactions also occur in plant cells. However, it cannot completely be excluded that a linker protein such as COP1 connects crys with SPAs under these conditions. Our FRET-FLIM studies clearly showed that cry2 and SPA1 bind directly to each other in the nuclei of living cells. However, using this assay we could not see interaction of cry2 with SPA2-4 (Figure 6). This negative result for SPA2-4 can be explained by their less robust interaction with cry2 seen in yeast two-hybrid interaction studies (Zuo et al., 2011). To find further evidence for or against direct interaction of cry2 with the members of the SPA

quartet, we used Co-IP studies with recombinant 6×His-tagged cry2 protein as bait and in vitro–translated and transcribed [^{35}S] Met-labeled SPA proteins. We used this approach mainly because the correct chromophore binding and a proper photocycle of the recombinant cry2 expressed in insect cells can be tested spectroscopically (Banerjee et al., 2007). The cry2 sample used in our Co-IP studies had indeed properly bound FAD and was photoactive (see Supplemental Figure 10A online). We immunoprecipitated the proteins with anti-His-tag antibodies against the His-tag positioned at the N terminus of cry2, which is, based on the cry1 structure (Brautigam et al., 2004), flexible and thus accessible to the antibody as verified in control immunoprecipitations (see Supplemental Figures 10B and 10C online). The observed signals for SPA2 and SPA3 in the autoradiogram after Co-IP are most likely unspecific because they are of the same intensity in the absence or presence of cry2 (Figures 7A and 7B). By contrast, we observed signals for SPA1 and SPA4 in the Co-IPs upon addition of cry2 that were completely missing in the assays without cry2 (Figures 7A and 7B). The intensity of these signals seemed not to be influenced by the applied white light. By contrast, a clear stimulation of cry2-SPA1 interaction by blue light was observed before in yeast two-hybrid and Co-IP studies (Zuo et al., 2011) However, we cannot exclude that at least some of the recombinant cry2 remained in the signaling state under our applied red light conditions, thus allowing interaction with SPA1 and SPA4. Consistent with this conclusion is the observation that the cry2–CIB1 interaction was likewise seen in the red light controls although stimulated by white light (Figure 7D). Further support for the specificity of cry2–SPA1 interaction came from negative controls with recombinant *E. coli* DNA photolyase as the bait protein. We used this enzyme as a control because of its high structural similarity with cry1 (Brautigam et al., 2004) and, thus, most likely also with cry2. The employed DNA photolyase, which was used at the same concentration as cry2, contained FAD and was photoactive (see Supplemental Figure 10A online). None of the tested proteins (CIB1 and SPA1) that interacted with cry2 gave a specific signal with the DNA photolyase (Figure 7E). In summary, our FRET-FLIM and Co-IP studies showed that SPA1 and SPA4 physically interact with cry2. cry2 is degraded in nuclear protein complexes (i.e., in nuclear bodies) (Yu et al., 2009). Based on our findings and the observation that the SPA1-cry2 complex binds COP1 more tightly than cry2 alone (Zuo et al., 2011), we suggest that only the heterotrimeric SPA1-cry2-COP1 complex, which is localized in nuclear bodies, allows efficient degradation of cry2. SPA2-SPA4 can substitute the lack of SPA1 but it is not clear yet whether one cry2 molecule binds the SPAs individually or even in a higher order complex.

METHODS

Plant Materials

The *Arabidopsis thaliana* mutants *phyA-211*, *cop1-6*, *spa1-7/2-1/4-1*, *spa1-7/3-1/4-1 spa1-7/2-1/3-1*, *spa1-7/2-1/3-1/4-1 spa1-7*, and *spa2-1/3-1/4-1* in the Columbia ecotype background have been described (McNellis et al., 1994; Reed et al., 1994; Laubinger et al., 2004; Fittinghoff et al., 2006). The mutants *phyA-412 cry1-304 cry2-1*, *cry1-1 cry2* (*fha-1*), *phyA-201*, and *phyB-5* in the L*er* ecotype background have been described by Reed et al. (1993), Yanovsky et al. (2000), and Mockler et al. (2003). The mutants *phyA-101*, *spa1-2*, and *phyA-101 spa1-2* in the RLD ecotype are described by Dehesh et al. (1993) and Hoecker et al. (1998).

Growth Conditions, Light Sources, Hypocotyl Measurements, and Proteasome Inhibitors

Arabidopsis seeds were surface sterilized with 25% bleach (sodium hypochlorite; 12% Cl) and 0.05% Triton X-100 for 10 min, followed by washing five times with distilled water. Seeds were plated on 0.5× Murashige and Skoog medium (Duchefa) without Suc or on three layers of Whatman paper soaked with distilled water for RNA isolation. After stratification for 4 d at 4°C in the dark, germination was induced by exposing seeds to white light for 4 h at 22°C. For analyzing cry2 protein and *CRY2* transcript levels, plates were kept after induction of germination for 4 d in the dark at 22°C and exposed afterwards to continuous blue, red, or far-red light or kept in darkness for 2 h. Plates for hypocotyl growth inhibition measurements were exposed directly after stratification to the dark, or to blue, red, or blue plus red light for 96 h.

Seedlings were exposed to light-emitting diode sources (CLF Plant Climatics) with emission maxima of λ_{max} 471 nm (blue light), λ_{max} 675 nm (red light), and λ_{max} 748 nm (far-red light). Fluence rates were determined using an Optometer P-2000 spectroradiometer (Gigahertz Optik), and light intensities were adjusted to the required fluence rates using a gray filter. For determination of cry2 protein and *CRY2* transcript levels, plant material was harvested under safe light (dim green light) and immediately shock-frozen in liquid nitrogen. For quantification of hypocotyl growth inhibition, seedlings were photographed using a Nikon Coolpix 5000 digital camera, and hypocotyl lengths were determined using Image J 1.40 (National Institutes of Health). For treatments with proteasome inhibitors, seedlings kept in the dark for 96 h after stratification were preincubated for 2 h in the dark either in a mixture of proteasome inhibitors in 2% DMSO or in 2% DMSO as a mock control. Afterwards, seedlings were exposed for 2 h to blue light (λ_{max} = 471 nm, 30 μmol m^{-2} s^{-1}) or kept for the same time in the dark and then immediately frozen in liquid nitrogen. The mixture of proteasome inhibitors contained ALLN, MG132, MG115, and PS1 (Merck), each at 50 μM.

Protein Extraction and Quantification of Proteins by Immunoblot Analysis

Plant material was pulverized in liquid nitrogen using an MM200 cell mill (Retsch), and the frozen powder was resuspended in extraction buffer (10% trichloroacetic acid, 90% acetone, and 0.07% β-mercaptoethanol). After three washing steps in acetone containing 0.07% β-mercaptoethanol, the pellets were resuspended in 1× SDS sample buffer, sonicated, and boiled for 5 min at 95°C. Equal amounts (20 μg) of protein extracts were subjected to SDS-PAGE and blotted onto nitrocellulose membranes. For immunodetection, polyclonal anti-cry2 antibody raised in rabbits and monoclonal mouse anti-α-tubulin antibody (Sigma-Aldrich) together with the secondary fluorophore-labeled antibodies IRDye 680 goat-anti-mouse IgG and IRDye 800CW goat-anti-rabbit IgG (Li-Cor) were applied using the Odyssey infrared imaging system (Li-Cor). Signal intensities of cry2 and α-tubulin were calculated by the Odyssey software. The quantified signals were normalized to the mean background. The cry2 signal was normalized against the α-tubulin signal in the same lane. The level of cry2 in the dark sample of each genotype was set as 100%.

RNA Isolation and Quantitative RT-PCR

For quantitative real-time PCR, total RNA was isolated from *Arabidopsis* seedlings using the RNeasy plant mini kit (Qiagen). Prior to RT-PCR, isolated RNA

was treated with Turbo DNase (Ambion) for elimination of genomic DNA. cDNA was synthesized using the first-strand cDNA kit (Fermentas). Every cDNA reaction was checked for contamination by residual genomic DNA in an additional PCR reaction using the UBQ real-time primers. Quantitative PCR was performed using the SensiFAST SYBR No-ROX kit (Bioline) with a Mastercycler ep Realplex apparatus (Eppendorf) with the following program: 95°C 2 min, 95°C 5 s, 60°C 10 s, 72°C 20 s, 40 cycles. The primers used for *CRY2* were forward (5′-GCTTTGCTGTGAAGTTTCTTCTCC-3′) and reverse (5′-GCCTTGTAACGCGG-GATTGTC-3′), and for *UBQ* forward (5′-CGGGAAAGACGATTACTCTTGAGG-3′) and reverse (5′-GCAAGAGTTCTGCCATCCTCC-3′). The relative *CRY2* transcript levels were normalized against the *UBQ* signals according to the $2^{-\Delta\Delta Ct}$ (cycle threshold) method (Livak and Schmittgen, 2001).

Constructs used for *Agrobacterium tumefaciens*–Mediated Tobacco Transformation

Design of full-length open reading frame (ORF) constructs of *SPA1* and *SPA2-4* in the gateway entry vector pENTR/D-TOPO (Invitrogen) has been described before (Laubinger et al., 2006; Zhu et al., 2008). Full-length ORF of *CRY2* without stop codon was PCR amplified from a cDNA plasmid with primers forward (5′-CACCATGAAGATGGACAAAAAGACTATAG-3′) and reverse (5′-TTGGCAACCATTTTTTCCCAAAC-3′). Full-length ORF of *CIB1* without stop codon was RT-PCR amplified from total RNA isolated from *Arabidopsis* Col-0 wild type by primers forward (5′-CACCATGA-ATGGAGCTATAGGAGGTGAC-3′) and reverse (5′-AACTCCTAAATTG-CCATAGAGATTC-3′). *CRY2* and *CIB1* PCR products were introduced in the entry pENTR/D-TOPO vector and correctness of the ORFs verified by sequencing. Transfer of these ORFs from the entry to the destination vectors was done using Gateway LR Clonase II Enzyme Mix (Invitrogen). The following plant binary destination vectors were used: pB7RWG2 C termini and pB7RWG2 N termini (Karimi et al., 2002) yielding in-frame fusions of the ORFs with RFP at their C (X-RFP) or N terminus (RFP-X), respectively. Expression in these vectors is driven by the cauliflower mosaic virus 35S promoter. pUGT1 and pUGT2 (Grefen et al., 2010) yielded in-frame fusions of the ORFs with mGFP5 at their C terminus (X-GFP) or N terminus (GFP-X), respectively. In pUGT vectors, expression is driven by the *Arabidopsis Ubiquitin 10* promoter. For SPAs, fusions with the fluorescent reporters were only made at the N termini of the SPA proteins since previous studies showed that they do not tolerate C-terminal fusions.

Transient Transformation of *Nicotiana benthamiana* leaves

After 4 to 6 weeks of cultivation in growth chambers (temperature 26°C day/19°C night, humidity 62%, 14 h white light) leaves of *N. benthamiana* plants were transformed with *Agrobacterium* strain GV3101 pMP90 (Schütze et al., 2009). Infiltration occurred in the adaxial sides of the leaves. The p19 protein from tomato bushy stunt virus was used for suppression of transgene silencing (Voinnet et al., 2000). Transformation of the different expression vectors encoding the fusion proteins was accomplished as described (Grefen et al., 2008).

Confocal Laser Scanning Microscopy and FRET-FLIM Studies

Three days after infiltration, the transient expression and localization of the fusion proteins in plant epidermal leaf cells were detected using confocal laser scanning microscopy. Afterwards some plant material was harvested followed by protein extraction for immunoblot analysis. In vivo interaction studies of the full-length fusion proteins were measured by FRET-FLIM with a confocal stage scanning microscope according to Wanke et al. (2011). For each tested combination of fusion proteins, three measurements of fluorescence lifetime decays were recorded and mean values estimated.

In Vitro Co-IP Assay

Some constructs used for in vitro transcription and translation have been described previously: SPA1 and GAD-COP1 (Hoecker and Quail, 2001), SPA2 (Laubinger et al., 2004), and SPA3 and SPA4 (Laubinger and Hoecker, 2003). The construct encoding full-length CIB1 in a modified pBS-*35S-AlaRLUC* vector (Subramanian et al., 2004) was available; we removed the ORF of RLUC by restriction with *Not*I and *Xba*I and replaced it by a c-Myc epitope-coding region containing a stop codon. The c-Myc epitope was generated by annealing of the two 41-mers 5′-GGCCGC-TGAGCAAAAGTTGATTTCTGAGGAGGATCTTTAGT-3′ and 5′-CTAGAC-TAAAGATCCTCCTCAGAAATCAACTTTTGCTCAGC-3′, which provided a double-stranded c-Myc epitope coding region with a *Not*I overhang at the 5′ end and an *Xba*I overhang at the 3′ end for ligation into the *Not*I-*Xba*I–restricted pBS-*35S-AlaRLUC* vector, replacing RLUC. CIB1-c-Myc was cut out of this modified pBS-*35S* vector using *Nco*I and *Bam*HI and inserted into the target vector pET-15b(+) (Novagen). The full-length coding region of *CIB1* was amplified with *pfu* DNA polymerase (Fermentas) from Col-O cDNA using primers 5′-CCATGGCCATGAATGG-AGCTATAGGAG-3′ and 5′-GCGGCCGCAACTCCTAAATTGCCATAG-3′, which contained a restriction site (underlined) for *Nco*I and *Not*I, respectively. After subcloning of the PCR product into the pGEM-T vector (Promega), the PCR product was verified by sequencing.

Prey proteins were expressed from the T7 promoters in the presence of [^{35}S]Met (Hartmann Analytic) using the TnT reticulocyte in vitro transcription/translation system (Promega) according to the manufacturer's instructions. The genes encoding the bait proteins His-cry2 and His-PHR (*Escherichia coli* DNA photolyase) were expressed, and the proteins were purified as described (Banerjee et al., 2007; Moldt et al., 2009).

For Co-IP, 50 μL of Dynabeads Protein G (Invitrogen) was incubated with 2.5 μg of monoclonal antibody against the 6×His-tag (Clontech-Takara Bio Europe) in binding/wash buffer (Immunoprecipitation Kit-Dynabeads Protein G; Invitrogen) in a total volume of 250 μL for 1 h at 4°C with mixing by rotation. In parallel, 10 μL of each TnT-produced prey protein was incubated in the absence or presence of 2 μg of either His-cry2 or His-PHR in a total volume of 100 μL in binding buffer (200 mM Tris, pH 7.5, 150 mM NaCl, 1 mM DTT, and 0.1% Tween 20) with Complete EDTA-free protease inhibitors (Roche). The magnetic beads were washed three times with 200 μL of wash buffer, and each prey protein sample (preincubated with or without bait) was individually added to the pre-incubated bead samples. Samples were further incubated for 1 h at 4°C with mixing by rotation, and the beads were collected and washed three times with 200 μL of wash buffer. Afterwards, the beads were re-suspended and boiled in 25 μL of 1× SDS sample buffer. The Co-IP fractions and 2 μL of each TnT reaction (also in 25 μL of 1× SDS sample buffer) were separated by SDS-PAGE, and signals were detected with a Storm 860 PhosphorImager (Molecular Dynamics).

Accession Numbers

Sequence data of genes encoding the proteins studied in this article can be found in the Arabidopsis Genome Initiative or GenBank/EMBL databases under the following accession numbers: CIB1, At4g34530; COP1, At2g32950; CRY2, At1g04400; PHYA, At1g09570; PHYB, At2g18790; SPA1, At2g46340; SPA2, At4g11110; SPA3, At3g15354; and SPA4, At1g53090.

Supplemental Data

The following materials are available in the online version of this article.

Supplemental Figure 1. Calibration Curves for CRY2 and α-Tubulin Signals in Relation to the Amount of Total Protein Loaded on Each Lane.

Supplemental Figure 2. Immunoblots Showing Blue Light (λ_{max} = 471 nm) Fluence Rate–Dependent Degradation of CRY2 in the Wild Type and Various Mutants in Different Backgrounds.

Supplemental Figure 3. *CRY2* Transcript Levels in Wild-Type, *spa1/2/4*, and *phyA* Mutant Seedlings.

Supplemental Figure 4. CRY2 Degradation in the Presence of Proteasome Inhibitors.

Supplemental Figure 5. Immunoblot of Protein Extracts from Seedlings Exposed to Red Light or Far-Red Light and Probed in Parallel with Anti-cry2 and Antitubulin Antibodies.

Supplemental Figure 6. Dose–Response Curve of CRY2 Degradation in Col-0, L*er*, and RLD Wild Types.

Supplemental Figure 7. Fluence Rate–Dependent Degradation of CRY2 in Wild-Type, *phyA-101*, *spa1-2*, and *phyA-101 spa1-2* Mutant Seedlings.

Supplemental Figure 8. Dose–Response Curve of Hypocotyl Growth Inhibition under Blue Light.

Supplemental Figure 9. Immunoblots Showing the Expression of Full-Length Fusions of CRY2, CIB1, and SPA1-SPA4 with Fluorescent Proteins.

Supplemental Figure 10. Characterization of Bait Proteins Used for in Vitro Coimmunoprecipitation Studies.

Supplemental Figure 11. Hypocotyl Growth Inhibition of Various Photoreceptor and *spa* Mutants.

Supplemental References 1. Supplemental References for Supplemental Figure 1.

ACKNOWLEDGMENTS

We thank Margaret Ahmad for providing anti-cry2 antibody and Agnes Damm and Elvira Happel for technical assistance. This work was supported by the German Research Foundation to A.B. (Deutsche Forschungsgemeinschaft Grant BA 985/11-1).

AUTHOR CONTRIBUTIONS

A.B., U.H, K.H., and F.S. designed the research. G.W., S.z.O.-K., M.H., and C.O. performed the research. A.B., F.S., K.H., G.W., and U.H. analyzed the data. U.H., K.H., and F.S. contributed new analytic and computational tools. A.B., U.H., and K.H. wrote the article.

Received March 14, 2012; revised May 10, 2012; accepted May 31, 2012; published June 26, 2012.

REFERENCES

Ahmad, M., and Cashmore, A.R. (1993). HY4 gene of *A. thaliana* encodes a protein with characteristics of a blue-light photoreceptor. Nature **366:** 162–166.

Ahmad, M., Jarillo, J.A., and Cashmore, A.R. (1998). Chimeric proteins between cry1 and cry2 *Arabidopsis* blue light photoreceptors indicate overlapping functions and varying protein stability. Plant Cell **10:** 197–207.

Banerjee, R., Schleicher, E., Meier, S., Viana, R.M., Pokorny, R., Ahmad, M., Bittl, R., and Batschauer, A. (2007). The signaling state of Arabidopsis cryptochrome 2 contains flavin semiquinone. J. Biol. Chem. **282:** 14916–14922.

Batschauer, A. (1993). A plant gene for photolyase: An enzyme catalyzing the repair of UV-light-induced DNA damage. Plant J. **4:** 705–709.

Bayram, O., Biesemann, C., Krappmann, S., Galland, P., and Braus, G.H. (2008). More than a repair enzyme: *Aspergillus nidulans* photolyase-like CryA is a regulator of sexual development. Mol. Biol. Cell **19:** 3254–3262.

Bouly, J.P., Giovani, B., Djamei, A., Mueller, M., Zeugner, A., Dudkin, E.A., Batschauer, A., and Ahmad, M. (2003). Novel ATP-binding and autophosphorylation activity associated with Arabidopsis and human cryptochrome-1. Eur. J. Biochem. **270:** 2921–2928.

Bouly, J.P., Schleicher, E., Dionisio-Sese, M., Vandenbussche, F., Van Der Straeten, D., Bakrim, N., Meier, S., Batschauer, A., Galland, P., Bittl, R., and Ahmad, M. (2007). Cryptochrome blue light photoreceptors are activated through interconversion of flavin redox states. J. Biol. Chem. **282:** 9383–9391.

Brautigam, C.A., Smith, B.S., Ma, Z., Palnitkar, M., Tomchick, D.R., Machius, M., and Deisenhofer, J. (2004). Structure of the photolyase-like domain of cryptochrome 1 from *Arabidopsis thaliana*. Proc. Natl. Acad. Sci. USA **101:** 12142–12147.

Brudler, R., Hitomi, K., Daiyasu, H., Toh, H., Kucho, K., Ishiura, M., Kanehisa, M., Roberts, V.A., Todo, T., Tainer, J.A., and Getzoff, E.D. (2003). Identification of a new cryptochrome class. Structure, function, and evolution. Mol. Cell **11:** 59–67.

Brunelle, S.A., Starr Hazard, E., Sotka, E.E., and Van Dolah, F.M. (2007). Characterization of a dinoflagellate Cryptochrome blue-light receptor with a possible role in a circadian control of the cell cycle. J. Phycol. **42:** 509–518.

Cashmore, A.R. (2003). Cryptochromes: Enabling plants and animals to determine circadian time. Cell **114:** 537–543.

Cashmore, A.R., Jarillo, J.A., Wu, Y.J., and Liu, D. (1999). Cryptochromes: Blue light receptors for plants and animals. Science **284:** 760–765.

Chaves, I., Pokorny, R., Byrdin, M., Hoang, N., Ritz, T., Brettel, K., Essen, L.O., van der Horst, G.T., Batschauer, A., and Ahmad, M. (2011). The cryptochromes: Blue light photoreceptors in plants and animals. Annu. Rev. Plant Biol. **62:** 335–364.

Clough, R.C., Jordan-Beebe, E.T., Lohman, K.N., Marita, J.M., Walker, J.M., Gatz, C., and Vierstra, R.D. (1999). Sequences within both the N- and C-terminal domains of phytochrome A are required for P_{FR} ubiquitination and degradation. Plant J. **17:** 155–167.

Clough, R.C., and Viestra, R.D. (1997). Phytochrom degradation. Plant Cell Environ. **20:** 713–721.

Dehesh, K., Franci, C., Parks, B.M., Seeley, K.A., Short, T.W., Tepperman, J.M., and Quail, P.H. (1993). *Arabidopsis* HY8 locus encodes phytochrome A. Plant Cell **5:** 1081–1088.

Duek, P.D., Elmer, M.V., van Oosten, V.R., and Fankhauser, C. (2004). The degradation of HFR1, a putative bHLH class transcription factor involved in light signaling, is regulated by phosphorylation and requires COP1. Curr. Biol. **14:** 2296–2301.

El-Din El-Assal, S., Alonso-Blanco, C., Peeters, A.J., Raz, V., and Koornneef, M. (2001). A QTL for flowering time in Arabidopsis reveals a novel allele of CRY2. Nat. Genet. **29:** 435–440.

Exner, V., Alexandre, C.M., Rosenfeldt, G., Alfarano, P., Nater, M., Caflisch, A., Gruissem, W., Batschauer, A., and Hennig, L. (2010). A gain-of-function mutation of Arabidopsis cryptochrome1 promotes flowering. Plant Physiol. **154:** 1633–1645.

Fittinghoff, K., Laubinger, S., Nixdorf, M., Fackendahl, P., Baumgardt, R.L., Batschauer, A., and Hoecker, U. (2006).

Functional and expression analysis of Arabidopsis SPA genes during seedling photomorphogenesis and adult growth. Plant J. **47:** 577–590.

Folta, K.M., Pontin, M.A., Karlin-Neumann, G., Bottini, R., and Spalding, E.P. (2003). Genomic and physiological studies of early cryptochrome 1 action demonstrate roles for auxin and gibberellin in the control of hypocotyl growth by blue light. Plant J. **36:** 203–214.

Froehlich, A.C., Chen, C.H., Belden, W.J., Madeti, C., Roenneberg, T., Merrow, M., Loros, J.J., and Dunlap, J.C. (2010). Genetic and molecular characterization of a cryptochrome from the filamentous fungus *Neurospora crassa*. Eukaryot. Cell **9:** 738–750.

Grefen, C., Donald, N., Hashimoto, K., Kudla, J., Schumacher, K., and Blatt, M.R. (2010). A ubiquitin-10 promoter-based vector set for fluorescent protein tagging facilitates temporal stability and native protein distribution in transient and stable expression studies. Plant J. **64:** 355–365.

Grefen, C., Städele, K., Růzicka, K., Obrdlik, P., Harter, K., and Horák, J. (2008). Subcellular localization and in vivo interactions of the *Arabidopsis thaliana* ethylene receptor family members. Mol. Plant **1:** 308–320.

Guo, H., Duong, H., Ma, N., and Lin, C. (1999). The Arabidopsis blue light receptor cryptochrome 2 is a nuclear protein regulated by a blue light-dependent post-transcriptional mechanism. Plant J. **19:** 279–287.

Guo, H., Yang, H., Mockler, T.C., and Lin, C. (1998). Regulation of flowering time by Arabidopsis photoreceptors. Science **279:** 1360–1363.

Harter, K., Meixner, A.J., and Schleifenbaum, F. (2012). Spectromicroscopy of living plant cells. Mol. Plant **5:** 14–26.

Hayama, R., and Coupland, G. (2004). The molecular basis of diversity in the photoperiodic flowering responses of Arabidopsis and rice. Plant Physiol. **135:** 677–684.

Heijde, M. et al. (2010). Characterization of two members of the cryptochrome/photolyase family from *Ostreococcus tauri* provides insights into the origin and evolution of cryptochromes. Plant Cell Environ. **33:** 1614–1626.

Hoang, N., Bouly, J.P., and Ahmad, M. (2008). Evidence of a light-sensing role for folate in Arabidopsis cryptochrome blue-light receptors. Mol. Plant **1:** 68–74.

Hoecker, U. (2005). Regulated proteolysis in light signaling. Curr. Opin. Plant Biol. **8:** 469–476.

Hoecker, U., and Quail, P.H. (2001). The phytochrome A-specific signaling intermediate SPA1 interacts directly with COP1, a constitutive repressor of light signaling in Arabidopsis. J. Biol. Chem. **276:** 38173–38178.

Hoecker, U., Tepperman, J.M., and Quail, P.H. (1999). SPA1, a WD-repeat protein specific to phytochrome A signal transduction. Science **284:** 496–499.

Hoecker, U., Xu, Y., and Quail, P.H. (1998). SPA1: A new genetic locus involved in phytochrome A-specific signal transduction. Plant Cell **10:** 19–33.

Jang, I.C., Henriques, R., Seo, H.S., Nagatani, A., and Chua, N.H. (2010). *Arabidopsis* PHYTOCHROME INTERACTING FACTOR proteins promote phytochrome B polyubiquitination by COP1 E3 ligase in the nucleus. Plant Cell **22:** 2370–2383.

Jang, I.C., Yang, J.Y., Seo, H.S., and Chua, N.H. (2005). HFR1 is targeted by COP1 E3 ligase for post-translational proteolysis during phytochrome A signaling. Genes Dev. **19:** 593–602.

Karimi, M., Inzé, D., and Depicker, A. (2002). GATEWAY vectors for Agrobacterium-mediated plant transformation. Trends Plant Sci. **7:** 193–195.

Kennedy, M.J., Hughes, R.M., Peteya, L.A., Schwartz, J.W., Ehlers, M.D., and Tucker, C.L. (2010). Rapid blue-light-mediated induction of protein interactions in living cells. Nat. Methods **7:** 973–975.

Kleine, T., Lockhart, P., and Batschauer, A. (2003). An Arabidopsis protein closely related to Synechocystis cryptochrome is targeted to organelles. Plant J. **35:** 93–103.

Kleiner, O., Kircher, S., Harter, K., and Batschauer, A. (1999). Nuclear localization of the Arabidopsis blue light receptor cryptochrome 2. Plant J. **19:** 289–296.

Lariguet, P., and Fankhauser, C. (2004). Hypocotyl growth orientation in blue light is determined by phytochrome A inhibition of gravitropism and phototropin promotion of phototropism. Plant J. **40:** 826–834.

Laubinger, S., Fittinghoff, K., and Hoecker, U. (2004). The SPA quartet: A family of WD-repeat proteins with a central role in suppression of photomorphogenesis in *Arabidopsis*. Plant Cell **16:** 2293–2306.

Laubinger, S., and Hoecker, U. (2003). The SPA1-like proteins SPA3 and SPA4 repress photomorphogenesis in the light. Plant J. **35:** 373–385.

Laubinger, S., Marchal, V., Le Gourrierec, J., Wenkel, S., Adrian, J., Jang, S., Kulajta, C., Braun, H., Coupland, G., and Hoecker, U. (2006). *Arabidopsis* SPA proteins regulate photoperiodic flowering and interact with the floral inducer CONSTANS to regulate its stability. Development **133:** 3213–3222. Erratum. Development **133:** 4608.

Leivar, P., Monte, E., Al-Sady, B., Carle, C., Storer, A., Alonso, J.M., Ecker, J.R., and Quail, P.H. (2008). The *Arabidopsis* phytochrome-interacting factor PIF7, together with PIF3 and PIF4, regulates responses to prolonged red light by modulating phyB levels. Plant Cell **20:** 337–352.

Lian, H.L., He, S.B., Zhang, Y.C., Zhu, D.M., Zhang, J.Y., Jia, K.P., Sun, S.X., Li, L., and Yang, H.Q. (2011). Blue-light-dependent interaction of cryptochrome 1 with SPA1 defines a dynamic signaling mechanism. Genes Dev. **25:** 1023–1028.

Lin, C., Yang, H., Guo, H., Mockler, T., Chen, J., and Cashmore, A.R. (1998). Enhancement of blue-light sensitivity of Arabidopsis seedlings by a blue light receptor cryptochrome 2. Proc. Natl. Acad. Sci. USA **95:** 2686–2690.

Liu, B., Liu, H., Zhong, D., and Lin, C. (2010). Searching for a photocycle of the cryptochrome photoreceptors. Curr. Opin. Plant Biol. **13:** 578–586.

Liu, B., Zuo, Z., Liu, H., Liu, X., and Lin, C. (2011). Arabidopsis cryptochrome 1 interacts with SPA1 to suppress COP1 activity in response to blue light. Genes Dev. **25:** 1029–1034.

Liu, H., Yu, X., Li, K., Klejnot, J., Yang, H., Lisiero, D., and Lin, C. (2008). Photoexcited CRY2 interacts with CIB1 to regulate transcription and floral initiation in Arabidopsis. Science **322:** 1535–1539.

Livak, K.J., and Schmittgen, T.D. (2001). Analysis of relative gene expression data using real-time quantitative PCR and the 2(-Delta Delta C(T)) Method. Methods **25:** 402–408.

Ma, L., Li, J., Qu, L., Hager, J., Chen, Z., Zhao, H., and Deng, X.W. (2001). Light control of *Arabidopsis* development entails coordinated regulation of genome expression and cellular pathways. Plant Cell **13:** 2589–2607.

Malhotra, K., Kim, S.T., Batschauer, A., Dawut, L., and Sancar, A. (1995). Putative blue-light photoreceptors from *Arabidopsis thaliana* and *Sinapis alba* with a high degree of sequence homology to DNA photolyase contain the two photolyase cofactors but lack DNA repair activity. Biochemistry **34:** 6892–6899.

McNellis, T.W., von Arnim, A.G., Araki, T., Komeda, Y., Miséra, S., and Deng, X.W. (1994). Genetic and molecular analysis of an allelic

series of cop1 mutants suggests functional roles for the multiple protein domains. Plant Cell **6:** 487–500.

Mockler, T., Yang, H., Yu, X., Parikh, D., Cheng, Y.C., Dolan, S., and Lin, C. (2003). Regulation of photoperiodic flowering by Arabidopsis photoreceptors. Proc. Natl. Acad. Sci. USA **100:** 2140–2145.

Moldt, J., Pokorny, R., Orth, C., Linne, U., Geisselbrecht, Y., Marahiel, M.A., Essen, L.O., and Batschauer, A. (2009). Photoreduction of the folate cofactor in members of the photolyase family. J. Biol. Chem. **284:** 21670–21683.

Müller, M., and Carell, T. (2009). Structural biology of DNA photolyases and cryptochromes. Curr. Opin. Struct. Biol. **19:** 277–285.

Ohgishi, M., Saji, K., Okada, K., and Sakai, T. (2004). Functional analysis of each blue light receptor, cry1, cry2, phot1, and phot2, by using combinatorial multiple mutants in Arabidopsis. Proc. Natl. Acad. Sci. USA **101:** 2223–2228.

Osterlund, M.T., Wei, N., and Deng, X.W. (2000). The roles of photoreceptor systems and the COP1-targeted destabilization of HY5 in light control of Arabidopsis seedling development. Plant Physiol. **124:** 1520–1524.

Phee, B.K., Park, S., Cho, J.H., Jeon, J.S., Bhoo, S.H., and Hahn, T.R. (2007). Comparative proteomic analysis of blue light signaling components in the Arabidopsis cryptochrome 1 mutant. Mol. Cells **23:** 154–160.

Pokorny, R., Klar, T., Hennecke, U., Carell, T., Batschauer, A., and Essen, L.O. (2008). Recognition and repair of UV lesions in loop structures of duplex DNA by DASH-type cryptochrome. Proc. Natl. Acad. Sci. USA **105:** 21023–21027.

Reed, J.W., Nagatani, A., Elich, T.D., Fagan, M., and Chory, J. (1994). Phytochrome A and phytochrome B have overlapping but distinct functions in Arabidopsis development. Plant Physiol. **104:** 1139–1149.

Reed, J.W., Nagpal, P., Poole, D.S., Furuya, M., and Chory, J. (1993). Mutations in the gene for the red/far-red light receptor phytochrome B alter cell elongation and physiological responses throughout *Arabidopsis* development. Plant Cell **5:** 147–157.

Saijo, Y., Sullivan, J.A., Wang, H., Yang, J., Shen, Y., Rubio, V., Ma, L., Hoecker, U., and Deng, X.W. (2003). The COP1-SPA1 interaction defines a critical step in phytochrome A-mediated regulation of HY5 activity. Genes Dev. **17:** 2642–2647.

Sancar, A. (2003). Structure and function of DNA photolyase and cryptochrome blue-light photoreceptors. Chem. Rev. **103:** 2203–2237.

Schütze, K., Harter, K., and Chaban, C. (2009). Bimolecular fluorescence complementation (BiFC) to study protein-protein interactions in living plant cells. Methods Mol. Biol. **479:** 189–202.

Searle, I., and Coupland, G. (2004). Induction of flowering by seasonal changes in photoperiod. EMBO J. **23:** 1217–1222.

Selby, C.P., and Sancar, A. (2006). A cryptochrome/photolyase class of enzymes with single-stranded DNA-specific photolyase activity. Proc. Natl. Acad. Sci. USA **103:** 17696–17700.

Seo, H.S., Yang, J.Y., Ishikawa, M., Bolle, C., Ballesteros, M.L., and Chua, N.H. (2003). LAF1 ubiquitination by COP1 controls photomorphogenesis and is stimulated by SPA1. Nature **423:** 995–999.

Shalitin, D., Yang, H., Mockler, T.C., Maymon, M., Guo, H., Whitelam, G.C., and Lin, C. (2002). Regulation of Arabidopsis cryptochrome 2 by blue-light-dependent phosphorylation. Nature **417:** 763–767.

Shalitin, D., Yu, X., Maymon, M., Mockler, T., and Lin, C. (2003). Blue light-dependent in vivo and in vitro phosphorylation of *Arabidopsis* cryptochrome 1. Plant Cell **15:** 2421–2429.

Sharrock, R.A., and Clack, T. (2002). Patterns of expression and normalized levels of the five Arabidopsis phytochromes. Plant Physiol. **130:** 442–456.

Shinomura, T., Nagatani, A., Hanzawa, H., Kubota, M., Watanabe, M., and Furuya, M. (1996). Action spectra for phytochrome A- and B-specific photoinduction of seed germination in *Arabidopsis thaliana*. Proc. Natl. Acad. Sci. USA **93:** 8129–8133.

Somers, D.E., Devlin, P.F., and Kay, S.A. (1998). Phytochromes and cryptochromes in the entrainment of the Arabidopsis circadian clock. Science **282:** 1488–1490.

Subramanian, C., Xu, Y., Johnson, C.H., and von Arnim, A.G. (2004). In vivo detection of protein-protein interaction in plant cells using BRET. Methods Mol. Biol. **284:** 271–286.

Tóth, R., Kevei, E., Hall, A., Millar, A.J., Nagy, F., and Kozma-Bognár, L. (2001). Circadian clock-regulated expression of phytochrome and cryptochrome genes in Arabidopsis. Plant Physiol. **127:** 1607–1616.

Valverde, F., Mouradov, A., Soppe, W., Ravenscroft, D., Samach, A., and Coupland, G. (2004). Photoreceptor regulation of CONSTANS protein in photoperiodic flowering. Science **303:** 1003–1006.

Voinnet, O., Lederer, C., and Baulcombe, D.C. (2000). A viral movement protein prevents spread of the gene silencing signal in *Nicotiana benthamiana*. Cell **103:** 157–167.

Wang, H., Ma, L.G., Li, J.M., Zhao, H.Y., and Deng, X.W. (2001). Direct interaction of Arabidopsis cryptochromes with COP1 in light control development. Science **294:** 154–158.

Wanke, D., Hohenstatt, M.L., Dynowski, M., Bloss, U., Hecker, A., Elgass, K., Hummel, S., Hahn, A., Caesar, K., Schleifenbaum, F., Harter, K., and Berendzen, K.W. (2011). Alanine zipper-like coiled-coil domains are necessary for homotypic dimerization of plant GAGA-factors in the nucleus and nucleolus. PLoS ONE **6:** e16070.

Wu, G., and Spalding, E.P. (2007). Separate functions for nuclear and cytoplasmic cryptochrome 1 during photomorphogenesis of Arabidopsis seedlings. Proc. Natl. Acad. Sci. USA **104:** 18813–18818.

Yang, H.Q., Tang, R.H., and Cashmore, A.R. (2001). The signaling mechanism of Arabidopsis CRY1 involves direct interaction with COP1. Plant Cell **13:** 2573–2587.

Yang, H.Q., Wu, Y.J., Tang, R.H., Liu, D., Liu, Y., and Cashmore, A.R. (2000). The C termini of Arabidopsis cryptochromes mediate a constitutive light response. Cell **103:** 815–827.

Yang, J., Lin, R., Sullivan, J., Hoecker, U., Liu, B., Xu, L., Deng, X.W., and Wang, H. (2005). Light regulates COP1-mediated degradation of HFR1, a transcription factor essential for light signaling in *Arabidopsis*. Plant Cell **17:** 804–821.

Yanovsky, M.J., and Kay, S.A. (2002). Molecular basis of seasonal time measurement in Arabidopsis. Nature **419:** 308–312.

Yanovsky, M.J., Mazzella, M.A., and Casal, J.J. (2000). A quadruple photoreceptor mutant still keeps track of time. Curr. Biol. **10:** 1013–1015.

Yu, X., Klejnot, J., Zhao, X., Shalitin, D., Maymon, M., Yang, H., Lee, J., Liu, X., Lopez, J., and Lin, C. (2007). *Arabidopsis* cryptochrome 2 completes its posttranslational life cycle in the nucleus. Plant Cell **19:** 3146–3156.

Yu, X., Sayegh, R., Maymon, M., Warpeha, K., Klejnot, J., Yang, H., Huang, J., Lee, J., Kaufman, L., and Lin, C. (2009). Formation of nuclear bodies of *Arabidopsis* CRY2 in response to blue light is associated with its blue light-dependent degradation. Plant Cell **21:** 118–130.

Zhu, D., Maier, A., Lee, J.H., Laubinger, S., Saijo, Y., Wang, H., Qu, L.J., Hoecker, U., and Deng, X.W. (2008). Biochemical characterization of *Arabidopsis* complexes containing CONSTITUTIVELY PHOTOMORPHOGENIC1 and SUPPRESSOR OF PHYA proteins in light control of plant development. Plant Cell **20:** 2307–2323.

Zuo, Z., Liu, H., Liu, B., Liu, X., and Lin, C. (2011). Blue light-dependent interaction of CRY2 with SPA1 regulates COP1 activity and floral initiation in Arabidopsis. Curr. Biol. **21:** 841–847.